

# Simulations of an ultracold, neutral plasma with equal masses

F. Robicheaux

*Department of Physics, Purdue University, West Lafayette, Indiana 47907, USA\**

B. J. Bender and M. A. Phillips

*Department of Physics, Auburn University, AL 36849-5311*

(Dated: May 9, 2018)

The results of a theoretical investigation of an ultracold, neutral plasma composed of equal mass positive and negative charges are reported. In our simulations, the plasma is created by the fast dissociation of a neutral particle. The temperature of the plasma is controlled by the relative energy of the dissociation. We studied the early time evolution of this system where the initial energy was tuned so that the plasma is formed in the strongly coupled regime. In particular, we present results on the temperature evolution and three body recombination. In the weakly coupled regime, we studied how an expanding plasma thermalizes and how the scattering between ions affects the expansion. Because the expansion causes the density to drop, the velocity distribution only evolves for a finite time with the final distribution depending on the number of particles and initial temperature of the plasma.

PACS numbers: 52.55.Dy, 34.80.Lx, 52.65.-y, 32.80.Ee

## I. INTRODUCTION

Ultracold and strongly coupled plasmas are non-traditional plasmas where the strong interparticle interactions can lead to collective behavior in the system.[1] Depending on the system, highly correlated behavior can emerge when the interaction energy exceeds the kinetic energy because the particles can only move in the classically allowed region of a highly structured potential energy surface. Experiments and calculations of ultracold plasmas consisting of electrons and positive atomic or molecular ions have demonstrated a wide variety of interesting effects.[1]

In this paper, we present the results of calculations of ultracold neutral plasmas where the masses of *all* particles are the same. There have been many experiments and simulations on electron-positron plasmas in many different situations (two of many examples are Refs. [2, 3]). However, the ultracold regime is largely unexplored. As discussed in Ref. [4], a possible way to create an ultracold, equal mass plasma is to dissociate cold molecules to a positive/negative ion pair (e.g.,  $\text{Rb}^+$  and  $\text{Rb}^-$  with a  $(M_- - M_+)/ (M_- + M_+) \sim 10^{-5}$ ).[5] The kinetic energy of the break up can be controlled by starting in different vibrational states of the molecule. For example, the Frank-Condon overlap region moves to larger  $R$  as the vibrational quantum number increases. With this picture in mind, we performed calculations where many pairs of oppositely charged ions are launched with opposite velocities so that the center of mass velocity of each pair is 0. Each pair has a random center of mass position. When the positive and negative ions separate to large distances, they can interact with all of the other

ions leading to a variety of effects.

One of the more interesting parameters that characterizes the plasma behavior is the Coulomb coupling parameter

$$\Gamma = \frac{e^2 / (4\pi\epsilon_0 a_{ws})}{k_B T} \quad (1)$$

where the Wigner-Seitz radius

$$a_{ws} = \left( \frac{3}{4\pi 2n} \right)^{1/3} \quad (2)$$

and  $e$  is the electron charge,  $k_B$  is Boltzmann's constant,  $n$  is the number density of one species, and  $T$  is the temperature; this expression has twice the density of the usual formula because both species can interact with the same footing. If  $\Gamma$  is larger than  $\sim 1$ , then the components of the plasma start displaying correlated motion and that component of the plasma is considered to be strongly coupled. If  $\Gamma$  is less than  $\sim 1$ , then the plasma is weakly coupled. In the weakly coupled limit, standard plasma concepts (e.g. Debye screening, electron-ion scattering, ...) and standard atomic concepts (e.g. three body recombination) are expected to be good approximations.

We present results of two qualitatively different aspects of an equal mass, ultracold neutral plasma. Previous calculations and experiments suggest that the early time behavior[6–8] and the late time expansion of the plasmas should be worth studying.[9–13]

The early time behavior can be interesting when the initial plasma temperature is low because a strongly coupled plasma heats up due to the energy released from three body recombination.[6–8, 10–13] For the typical ultracold plasma, two electrons scatter in the vicinity of a positive ion leading to one electron becoming bound while the second leaves with a larger energy. As seen

---

\*Electronic address: robichf@purdue.edu

in Refs. [7, 8], the electron coupling parameter decreases from  $\sim 1$  to  $\sim 0.6$  on a time scale of  $\sim 10$  plasma periods of the electron. Reference [7] presented calculations of the early time heating of the plasma due to this process for an ion mass substantially larger than the electron mass but much less than physical masses. Reference [8] revisited this system and calculated the heating as a function of the ion mass (Ref. [8], Fig. 2) and found that smaller ion masses gave lower electron temperatures. These results motivated us to study the early time behavior of initially strongly coupled plasmas when the mass of the positive charge equals that of the negative charge. In addition to the possible changes to the three body recombination and heating, we point out that the ion plasma period would be of order  $100\times$  longer than the electron plasma period. Thus, there would be an experimentally substantial time interval for studying neutral plasmas where both components have  $\Gamma \sim 1$ .

The other possibility for interesting physics is in the expansion of the plasma.[9, 11–13] For this investigation, we used plasma temperatures sufficiently high that we could treat the species as weakly coupled. In the usual ultracold plasmas, the electrons are confined by the space charge of the ions and the pressure from the electrons gives a radially outward force on the ions.[1, 6] During the expansion, the electron temperature drops substantially and this energy is converted to radial kinetic energy of the ions. For an equal mass plasma, this description of the expansion can not be correct; unlike the electron-ion plasma, the equal mass plasma could expand faster than the plasma properties can be established. The plasma period scales like  $n^{-1/2}$  where  $n$  is the density whereas the expansion time scales with  $L/v_{th} \propto LT^{-1/2}$  where  $L$  is a size scale of the plasma and  $T$  is the temperature of one of the components. Since these two time scales vary with completely different parameters, it should be possible to explore scenarios where there are many plasma oscillations before the plasma substantially expands. Since the two species start with the same temperature, the plasma expansion can not extract energy from the thermal motion. The dominant effects arise from the competition between particle scattering (which leads to thermalization and slows the expansion) and plasma expansion (which decreases the density and slows the particle scattering).

In all discussions below, the quoted density is the density of one species. The total density of particles is, of course, twice this value.

## II. NUMERICAL METHOD

We were interested in two qualitatively different types of behavior which required two different types of computational methods. For the early time behavior of a strongly coupled plasma, we needed to simulate the thermalization and evolution of the coupling parameter on a time scale less than 10 plasma periods. This required a method that computes the positions and velocities of all

the particles. For the late time behavior, we needed to simulate the thermalization and expansion of the plasma for the case of weak coupling. This required a method that could handle millions of particles over very long time scales but where only pair-wise collisions are relevant.

### A. Molecular dynamics method

The calculations for the early time behavior of a strongly coupled plasma used an adaptive steps-size, Runge-Kutta algorithm[14] to solve the classical equations of motion with wrap boundary condition for the forces. These calculations used the same method and programs as described in Ref. [8] Secs. 2 and 3 except the masses of the positive and negative particles are the same. All of the particles were contained within a cube of length  $L$  so that the number of positive particles divided by the volume equaled the target density. When a particle reached the edge of the cube, it was wrapped back into the cube; for example, if the  $x_j$  was larger than  $L$  then it was replaced by  $x_j - L$  before the next time step. We did not use a pure Coulomb force for the particles all of the way to zero separation. We derived the force from a spherically symmetric potential between particles  $i$  and  $j$  that had the form

$$PE_{ij} = \frac{q_i q_j}{4\pi\epsilon_0 \sqrt{r_{ij}^2 + (Ca_{ws})^2}} \quad (3)$$

where  $q_i$  is the charge of particle  $i$ ,  $r_{ij}$  is the separation of particles  $i$  and  $j$ ,  $a_{ws} = [3/(4\pi 2n)]^{1/3}$  is the Wigner-Seitz radius which is found from the number density  $n$ , and  $C$  is a constant substantially less than 1. We performed calculations for several values of  $C$  from 0.01 to 0.05 to determine the effect that the soft core had on the dynamics. The role that the constant  $C$  plays in the calculation are discussed below in the results of the different simulations. We emphasize that this form of the potential is a numerical device for speeding the calculation while keeping the physical result the same. In our simulations, we are calculating the behavior for a finite number of particles so the treatment of the boundary could be important. As is typical, we used a wrap boundary condition on a cube when computing the forces. When we computed the force or potential energy between two particles, we would use  $x_i - x_j$  if  $-L/2 \leq (x_i - x_j) \leq L/2$  but would use  $x_i - x_j + L$  if it was less than  $-L/2$  and  $x_i - x_j - L$  if it was greater than  $L/2$ . Similar definitions applied to the  $y$ - and  $z$ -components. As the number of particles in the simulation increases for a given density, the size of the cube increases and the effect of the edges becomes less. We checked convergence with respect to the cube size by comparing the results from different size runs.

The particles were initialized to mimic a sudden dissociation of positive and negative ions. Each pair of positive and negative ions were randomly placed within the cube. The initial separation of a positive-negative ion pair was

$a_{ws}/2500$ ; the separation vector for each pair was randomly chosen with a uniform distribution on a sphere. Their initial velocity vectors were chosen to be equal and opposite so the center of mass velocity was zero; their directions were chosen so they moved directly apart. The magnitude of velocity was chosen so that the energy of the pair would be  $2/3$  the temperature.

We made sure our reported results were converged with respect to the time step in the calculation. This was checked by increasing the accuracy parameter in the calculation. We checked that the results in our plots did not change and we checked that the total energy of the system drifted by less than a mK per particle.

### B. Fokker-Planck method

We also wanted to investigate how an experimentally sized system would thermalize and expand. For this situation, there could be millions of particles but we studied cases where the temperature was high enough that the plasma was only weakly coupled. These conditions suggest using a Fokker-Planck type method to include the effect of scattering on the motion. We simulated a case where the positive and negative ions have a Gaussian distribution in space but each pair is launched back-to-back. The plasma will maintain its spherical symmetry during the expansion. Because there could be different conditions in different radial regions we implemented a somewhat complex Fokker-Planck method. The method was nearly identical to that described for electron-electron scattering in Sec. IIIA of Ref. [15].

As in the previous section, the positive and negative particles are launched in pairs with 0 center-of-mass velocity. The pairs are launched with a fixed separation and speed. In the absence of scattering with other particles, *all* particles would have the same speed. The initial speed distribution is strongly peaked. Collisions broaden the distribution and, in the limit that the particles can scatter many times, the velocities will approach a Maxwell-Boltzmann distribution. The “temperature” quoted for each calculation is  $2/3$  the energy for each pair. The initial center of mass position for each pair is chosen randomly from a spherical Gaussian distribution proportional to  $\exp(-r^2/L_g^2)$  where the length scale

$$L_g = (N/\bar{n})^{1/3}/\sqrt{2\pi} \quad (4)$$

where  $\bar{n}$  is the average density and  $N$  is the number of positive (or negative) ions. The local (single species) density is  $n(r) = 2^{3/2}\bar{n} \exp(-r^2/L_g^2)$ .

For the Fokker-Planck simulation, we would first step every particle’s position using its velocity and then we would update the velocity using pairwise scattering between particles.[15] In this method, the local density is used to determine the scattering rate experienced by each particle Unlike the electron-electron scattering in Ref. [15], the ions in our plasma tend to stay near the

same ions once the expansion begins which led to numerical instabilities. We avoided this problem by computing the plasma density on a grid that evolved in time; the radial grid kept a fixed number of points but the spacing changed with the particle with the largest  $r$ :  $\delta r = \max(r)/N_r$  where the number of grid points,  $N_r$ , was fixed. As in Ref. [15], only particles with nearly the same  $r$  are allowed to scatter from each other.

There are three important parameters to check for convergence. The most important parameter to test is the time step. The probability for a pair to scatter during a time step is proportional to  $\delta t$ . If this probability becomes larger than  $\sim 0.1$  for a substantial fraction of the pairs, then the effect from scattering will be underestimated. Another parameter to check is the radial dependence of the density which determines how often an ion near a radius  $r$  will scatter. We compute the density by distributing particles on a radial grid. If the grid is too coarse, the density variation will not be as rapid as it should. If the grid is too fine, then the statistical noise from the finite number of particles in the calculation will give errors in the local density. Finally, we needed to only allow scattering between pairs of particles with small separation in  $r$ . This was accomplished in two steps. First a group of possible scatterers were randomly picked from the particles. Second, a scattering particle was picked and the particle in the scattering group with the closest  $r$  was used to scatter. Lastly, the particle pulled from the scattering group was replaced by another random particle. Ideally, the scattering group should consist of all particles but it would be prohibitively slow to search such a large list. We checked the convergence of the results with the size of the scattering group by doubling its size until the final results differed by less than 2%.

To test whether this method could give reasonable results, we performed molecular dynamics calculations with 6,400 positive and 6,400 negative ions and compared to the Fokker-Planck calculation. The comparison between these calculations are given in the results section below.

### III. SCALING

All of our calculations are purely classical which means that our results have exact scaling properties. Therefore, we can present our results for one specific choice of mass and density while varying the initial energy. These results will be applicable to other cases that have the same scaled parameters.

*Mass scaling.* All of the results presented below were obtained for the positive and negative charges each having the mass equivalent to one proton. To obtain the scaling relation, note that only the time and speed variables need to be scaled to obtain the same equations of motion. If you write  $t = \tilde{t}\sqrt{M/\tilde{M}}$ , you find that all of the velocities are scaled by the factor  $\sqrt{\tilde{M}/M}$  but *all*

other parameters (e.g. positions, energies, etc) are unchanged. As an example, if the only change is that the mass is larger by a factor of 16 while the initial density and energy are held fixed, then the same motion occurs but over a time scale a factor of 4 longer.

*Density scaling.* If the mass and charge are held fixed, the classical equations of motion exactly scale under the transformation

$$v = \alpha^{-1}\tilde{v} \quad r = \alpha^2\tilde{r} \quad t = \alpha^3\tilde{t} \quad (5)$$

where  $\alpha$  is a dimensionless scale factor. The energy scales as  $E = \alpha^{-2}\tilde{E}$  while the density scales as  $n = \alpha^{-6}\tilde{n}$ . Thus, we can explore different parameter regimes by either changing the initial energy or the initial density; it is not necessary to change both. The scaled energies and densities are related through  $n = \tilde{n}(E/\tilde{E})^3$  which means decreasing the energy by a factor of 2 while keeping the initial density fixed is equivalent to increasing the initial density by a factor of 8 while keeping the energy fixed.

#### IV. RESULTS

In this section, all of the calculations use a mass equal to that for one proton and an average (one-species) density of  $n = 10^9 \text{ cm}^{-3}$ . Since the masses are all equal, we use  $2n$  in all of the expressions for the plasma parameters. The plasma frequency  $\omega_p = \sqrt{2ne^2/M\epsilon_0} = 5.89 \times 10^7 \text{ rad/s}$  and the Wigner-Seitz radius is  $a_{ws} = (3/4\pi 2n)^{1/3} = 4.92 \text{ }\mu\text{m}$ . When computing the Coulomb coupling constant  $\Gamma = e^2/(4\pi\epsilon_0 a_{ws} k_B T)$  gives  $\Gamma = (3.39 K)/T$ .

##### A. Early time behavior of strongly coupled plasma

In this section, we present the results of the evolution of an ultracold plasma at early times. We performed convergence checks as in Ref. [8]. We found our results depended less on the soft core parameter  $C$  than in Ref. [8]; all of the results in this section used  $C = 0.01$  although they were nearly indistinguishable from the  $C = 0.02$  or  $0.03$ .

For this section, the particles are launched with an energy so that the average temperature for a diffuse plasma would be 1 K. The plasma should be strongly coupled with such a low temperature:  $\Gamma = 3.39$ . However, ultracold neutral plasmas consisting of electrons and ions do not exhibit strong coupling of electrons due to heating from three body recombination. References [7, 8] showed the temperature rise at early times (of order 10 plasma periods);  $\Gamma_e$  starts at  $\sim 1$  due to disorder induced heating over a time scale of  $\sim 1/\omega_p$  followed by a decrease to  $\sim 0.6$  over a time scale of  $\sim 10$  plasma periods. We expect a similar effect for equal mass plasmas because three body recombination should be important, but the role of the mass *will* change the results.

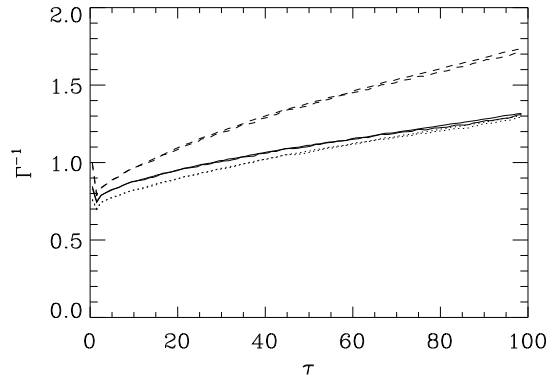


FIG. 1: Six calculations of the scaled temperature,  $\Gamma^{-1} = k_B T / [e^2 / (4\pi\epsilon_0 a_{ws})]$ , are shown as a function of the scaled time  $\tau = \omega_p t$ . The plasma parameters are in the text. The solid lines are when an ion closer to another ion than  $0.1a_{ws}$  were excluded from the calculation of the temperature and, for the dotted line, the exclusion region was  $0.2a_{ws}$ . The dashed line includes all ions, even those forming bound states. Each line type is actually two lines: one for a calculation using 800 particles of each sign and one for a calculation using 400 particles of each sign. The near equality of the calculations with 400 and 800 particles demonstrates the convergence.

Figure 1 shows the inverse of the coupling constant with time scaled by the plasma frequency. The  $\Gamma^{-1}$  is proportional to the temperature while quickly showing whether the plasma is strongly coupled. We defined the temperature to be  $2/3$  the average kinetic energy. One difficulty is in deciding which particles to include in the average kinetic energy. Reference [7] took all electrons that were not deeply bound to an ion and found their velocity distribution; they fitted this distribution to a Maxwell-Boltzmann distribution to obtain the temperature. Reference [8] obtained the temperature by using the equipartition theorem for electrons that were further than a specified distance from every ion; the distance we chose was either  $a_{ws}/10$  or  $a_{ws}/5$  (comparing the two calculations gives an estimate of the uncertainty of the temperature); they found this result agreed with the method of Ref. [7]. In Fig. 1, the dotted and solid lines correspond to the scaled temperature when the distance was chosen to be  $a_{ws}/5$  and  $a_{ws}/10$  respectively. The dashed line includes all particles but gives an unphysically high temperature due to “deeply” bound ion pairs.

The value of the plasma period can be used to convert the time axis to physical value. For protons, the final time is  $\simeq 1.7 \text{ }\mu\text{s}$ . For other ions, the time scale would increase by a factor of  $\sqrt{M_{ion}/M_{proton}}$  which could easily stretch the time scale to order  $10 \text{ }\mu\text{s}$ . This would be easily within the time scale of experimental probes (e.g. see Ref. [16]).

A Coulomb coupling parameter of  $\Gamma = 1$  is approximately the demarcation between a strongly or a weakly coupled plasma. The results in Fig. 1 are similar to those

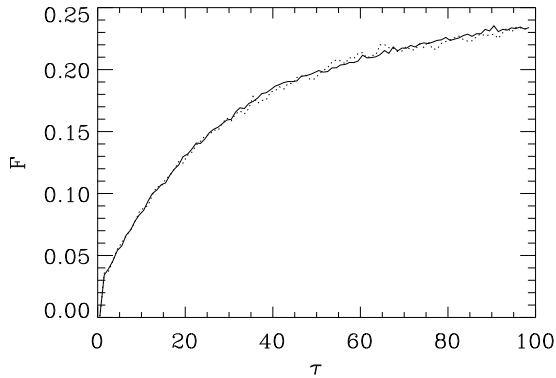


FIG. 2: Fraction of bound particles as a function of the scaled time  $\tau = \omega_p t$ . The solid line used 800 particles of each type while the dotted line used 400 particles of each type.

for electron-ion plasmas (e.g. Fig. 1 of Ref. [8]) but the coupling parameter for equal mass particles is somewhat larger than the electron-ion case. However, the electron component of the ultracold plasma is hard to probe and the total time scale for a duration like Fig. 1 would be  $\sim 60$  ns. Although the results for the equal mass plasma do not qualitatively differ from the electron-ion case, the equal mass plasma is worth studying because it seems possible to experimentally probe the equal mass plasma with parameters near that for strong coupling.

The heating in Fig. 1 is due to three body recombination, but the number of bound atoms can not be inferred from this data. Figure 2 shows the fraction of bound particles as a function of time for the plasma parameters of Fig. 1. For this plot, we defined a pair  $j$ - $j'$  as bound if the closest particle to  $j$  was  $j'$  for two times separated by  $1/\omega_p$  and the separation was less than  $a_{ws}/5$ . The results did not substantially change when the separation distance was less than  $a_{ws}/10$ .

Figure 2 shows that a substantial fraction of particles become bound over this time range. As might be expected, the fraction of bound pairs has a rapid initial increase followed by a much slower rise. This is expected because the three body recombination rate rapidly decreases with increasing temperature and is proportional to the square of the number of free particles. If the density drops by a factor of 0.8, then the recombination rate drops by the factor 0.64.

The center-of-mass speed of the bound pairs will be substantially less than that of the free particles. Therefore, it should be possible to detect the bound pairs by waiting for the free particles to expand out of the region where the plasma was created. Later, the particles can be dissociated and detected by ramping on an electric field.

In Fig. 1, we did *not* include the change to the Wigner-Seitz radius,  $a_{ws}$ , in the changing  $\Gamma$ . However, this change does not have a large effect. Changing the density

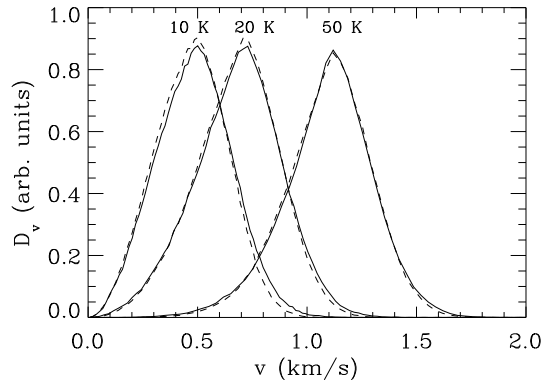


FIG. 3: The velocity distribution for an expanding plasma composed of 6,400 positive and 6,400 negative ions for three different temperatures. The final time for all calculations was 4 plasma periods, i.e.  $t_{fin} = 8\pi/\omega_p$ . The solid line is the result from the molecular dynamics calculation and the dashed line is the result of the Fokker-Planck calculation. The individual temperatures have been scaled to a peak of  $\sim 0.9$  but the relative scaling of the Fokker-Planck and molecular dynamics is held fixed.

by a factor of 0.77 changes  $a_{ws}$  by a factor of 1.09. This would increase the  $\Gamma^{-1}$  by the same factor of 1.09.

## B. Expanding Plasma

This section contains our results on how the ion-ion scattering affects the plasma expansion. If there were no scattering, then every ion would have the same speed. Since the particles start in a compact region, they would move approximately radially at late times with a speed  $v_{init}$ . This would give a radial shell of particles expanding with this speed. Collisions between ions could drastically change this picture. There is an interesting competition between scattering and plasma expansion. The scattering tends to delay the expansion. However, once the expansion is underway, the scattering rate quickly drops. Therefore, there is a well defined final velocity distribution that depends on the initial number and temperature of the particles. Since Coulomb collision rates decrease with temperature, the effects from scattering will be most pronounced at the lowest temperatures.

The collisions will tend to randomize the velocities, with more collisions tending to give a larger spread of velocities. In the limit of infinite collisions, the velocity distribution will go to a Maxwell-Boltzmann distribution. In terms of the distribution of speeds, the Maxwell-Boltzmann distribution is proportional to  $v^2 \exp(-Mv^2/[2k_B T])$  which has a peak at  $v = \sqrt{2k_B T/M}$ . The initial peak in speed is at  $v_{init} = \sqrt{3k_B T/M}$ . Thus, the collisions will move the peak in the distribution to smaller speeds while broad-

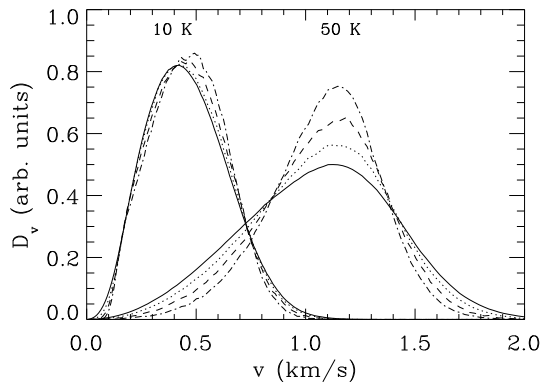


FIG. 4: The velocity distribution for an expanding plasma for different number of ions for two different temperatures. The final time for all calculations was  $6L_{g,max}/v_{init}$  where  $L_{g,max}$  was the  $L_g$  for the calculation with  $5.12 \times 10^6$  particles of each type. The solid line is for  $5.12 \times 10^6$ , the dotted line is for  $1.28 \times 10^6$ , the dashed line is for  $3.2 \times 10^5$  and the dot-dash line is for  $8 \times 10^4$  particles of each type. The individual temperatures have been scaled but the relative scaling within a temperature is held fixed.

ening the distribution. Another effect is that each collision changes the direction the particle is traveling. This will slow the initial expansion of the plasma because the particle motion will be more like a random walk. This slowing effect could be observable if the particle detector is close to the plasma because the delay could be a large fraction of the travel time.

Performing molecular dynamics calculations for  $10^5 - 10^6$  particles would be incredibly slow which is why we used a Fokker-Planck method to obtain the results in this section. Figure 3 shows a comparison between the two methods for a small enough number of particles where both methods can be used. The initial speed for 10, 20, and 50 K are 498, 704, and 1114 m/s respectively. All three distributions are peaked near these values but are substantially broadened. If these distributions were Maxwell-Boltzmann, the peaks would be at 407, 575, and 909 m/s respectively. As expected the 10 K distribution shows the largest spreading relative to the peak.

Most important is the comparison between the two methods. There is good agreement for the three different temperatures. The best agreement is for 50 K which we expected since this plasma is the best example of a weakly coupled plasma. We did not test calculations for temperatures lower than 10 K because the Coulomb coupling is becoming uncomfortably large,  $\Gamma = 0.34$ , at this temperature. In fact, the 10 K results have the largest disagreement. The Fokker-Planck calculations somewhat underestimate the high energy part of the distribution. However, this difference seems to be small enough that we can use this approximation to obtain the general behavior of the plasma expansion.

Figure 4 shows the velocity distribution for different

numbers of particles. The final time in all of the calculations is large enough that the plasma has expanded to the point where further changes in the velocity distribution are negligible. Each line type corresponds to a factor of 4 in the number of particles. The largest calculation had 5.12 million particles of each type while the smallest had 80 thousand. Note that even the smallest calculation has 10 times more particles than in Fig. 3. There are a few general trends worth noting.

One of the interesting features is that the peak of the 10 K distribution is moving to smaller  $v$  while the position of the peak of the 50 K distribution is nearly unchanged. In Fig. 3, the peak for all of the distributions was near the  $v_{init}$  for that temperature. It appears that the scattering leaves the position of the peak approximately unchanged until the width of the distribution becomes nearly equal to the value of the peak. Another interesting feature is how little the distributions change as more particles are added. Each line type corresponds to a factor of 4 in the number of particles which is a factor of  $4^{1/3} \simeq 1.6$  in the size of the plasma. If the plasma size increases by a factor of 1.6, the amount of time when collisions could happen increases by at least a factor of 1.6. (Since collisions slow the plasma expansion, the duration for possible collisions will increase somewhat faster than linearly with the plasma size.) Although each line type corresponds to another factor of 1.6 in plasma size, there is only  $\sim 10\%$  change in the 50 K distribution; the almost complete lack of change in the 10 K distribution, for the largest numbers, will be addressed below.

The speed distribution must have small  $v$  behavior proportional to  $v^2$  or a higher power. This masks one of the trends that arises because Coulomb scattering is larger at smaller relative energy. The high energy tail of the distribution is being filled more slowly than the low energy part. This is easiest to see in the 5.12 million calculation for 50 K (solid line). The distribution drops from the peak faster on the high energy side than the low energy side.

Figure 5 shows a comparison of the final speed distribution to a Maxwell-Boltzmann distribution. All of the Fokker-Planck calculations have  $5.12 \times 10^6$  particles of each type and, thus, should have the largest amount of scattering of our calculations. As expected, the 10 K distribution is most similar to the Maxwell-Boltzmann distribution while the 50 K distribution is least similar. This shows that the distribution does approach thermal for a large enough number of particles. The small changes in the 10 K distribution in Fig. 4 is because the distribution is nearly thermal.

The 20 K and 50 K distributions both show that the difference from a thermal distribution is more strongly pronounced on the high energy side of the peak compared to the low energy side because Coulomb collisions thermalize high energy particles slower than low energy particles.

Experimental results corresponding to Figs. 4 and 5 would be interesting. These plots are, in essence,

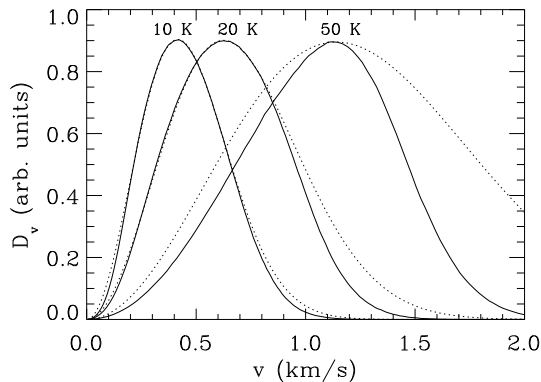


FIG. 5: The velocity distribution for an expanding plasma for three different temperatures. The final time was the same as Fig. 4. The Fokker-Planck calculations are the solid lines and have  $5.12 \times 10^6$  particles of each type. The dotted lines are Maxwell-Boltzmann distributions chosen to have a peak at the  $v$  from the Fokker-Planck calculation. All curves have been multiplied by a scaling constant so they all have the same height.

snapshots of how the Maxwell-Boltzmann distribution is reached in a plasma. By changing the number and/or energy of the plasma, there is direct control over the duration of the particle scattering. The final velocity distribution gives a direct test of our understanding of charged-particle scattering in a plasma.

## V. CONCLUSIONS

We have performed two types of calculations for ultracold neutral plasmas where all of the particles have the same mass. In our molecular dynamics calculations, we

investigated the initial heating and formation of bound states for a plasma that is strongly coupled initially. We found similar heating as observed in ion-electron calculations but the physical time scale is now of order 1-10  $\mu\text{s}$ . In our Fokker-Planck calculations, we studied the expansion and thermalization of particles of a weakly coupled plasma. Because the density drops with expansion, the collision rate rapidly drops and the velocity distribution stops evolving. We showed that the speed distribution approaches a Maxwell-Boltzmann distribution at low temperature and with enough particles; the largest differences are on the high energy side of the distribution.

There are several situations that we did not investigate due to the limitations of our computational tools. One interesting possibility would be to study this system in a strong magnetic field.[17] If the cyclotron radius of the motion becomes comparable to or smaller than the plasma size, there should be interesting modifications to the scattering. Also, there could be interesting plasma waves and instabilities because both species have the same mass which would argue that a plasma wave in one species will be degenerate with one in the other species. Another interesting possibility would be to study the expansion of a plasma that is initially strongly coupled. A final interesting possibility would be to include a direction distribution for the initial dissociation of charges; for example, there would be different scattering if the charges are launched mainly in the  $\pm z$ -direction than if they are launched in random directions as was done in our calculations.

We thank Phil Gould for interesting discussions that motivated us to study this system. This material is based upon work supported by the U.S. Department of Energy Office of Science, Office of Basic Energy Sciences Chemical Sciences, Geosciences, and Biosciences Division under Award Number de-sc0012193.

- 
- [1] T. Killian, T. Pattard, T. Pohl, and J. Rost, *Phys. Rep.* **449**, 77 (2007).
  - [2] R. G. Greaves and C. M. Surko, *Phys. Rev. Lett.* **75**, 3846 (1995).
  - [3] C. P. Ridgers, et al, *Phys. Rev. Lett.* **108**, 165006 (2012).
  - [4] A. Kirrander, S. Rittenhouse, M. Ascoli, E.E. Eyler, P.L. Gould, and H.R. Sadeghpour, *Phys. Rev. A* **87**, 031402 (2013).
  - [5] An example of ion-pair potential curves is T. Ban, R. Beuc. H. Skenderović and G. Pichler, *Europhys. Lett.* **66**, 485 (2004).
  - [6] T.C. Killian, M.J. Lim, S. Kulin, R. Dumke, S.D. Bergeson, and S.L. Rolston, *Phys. Rev. Lett.* **86**, 3759 (2001).
  - [7] S.G. Kuzmin and T.M. O'Neil, *Phys. Plasmas* **9**, 3743 (2002).
  - [8] K. Niffenegger, K.A. Gilmore, and F. Robicheaux, *J. Phys. B* **44**, 145701 (2011).
  - [9] S. Kulin, T.C. Killian, S.D. Bergeson, and S.L. Rolston, *Phys. Rev. Lett.* **85**, 318 (2000).
  - [10] S. Mazevet, L.A. Collins, and J.D. Kress, *Phys. Rev. Lett.* **88**, 055001 (2002).
  - [11] F. Robicheaux and J.D. Hanson, *Phys. Rev. Lett.* **88**, 055002 (2002).
  - [12] S.G. Kuzmin, and T.M. O'Neil, *Phys. Rev. Lett.* **88**, 065003 (2002).
  - [13] S.G. Kuzmin, and T.M. O'Neil, *Phys. Plasmas* **9**, 3743 (2002).
  - [14] W. H. Press, S. A. Teukolsky, W. T. Vetterling, and B. P. Flannery, *Numerical Recipes, 2nd Ed.*, Cambridge University Press NY (1992).
  - [15] F. Robicheaux and J.D. Hanson, *Phys. Plasmas* **10**, 2217 (2003).
  - [16] Y.C. Chen, C.E. Simien, S. Laha, P. Gupta, Y.N. Martinez, P.G. Mickelson, S.B. Nagel, and T.C. Killian, *Phys. Rev. Lett.* **93**, 265003 (2004).
  - [17] X.L. Zhang, R.S. Fletcher, and S.L. Rolston, **101**, 195002

(2008).